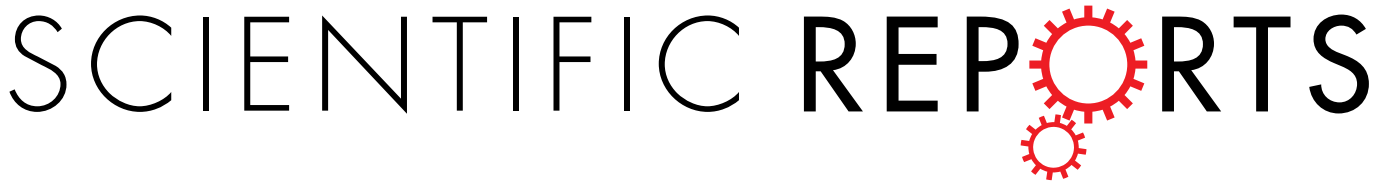

OPEN

Strongly polarizing weakly coupled ^{13}C nuclear spins with optically pumped nitrogen-vacancy center

Received: 30 May 2015
Accepted: 01 October 2015
Published: 02 November 2015

Ping Wang[1,2], Bao Liu[2] & Wen Yang[2]

Enhancing the polarization of nuclear spins surrounding the nitrogen-vacancy (NV) center in diamond has recently attracted widespread attention due to its various applications. Here we present an analytical formula that not only provides a clear physical picture for the recently observed polarization reversal of *strongly coupled* ^{13}C nuclei over a narrow range of magnetic field [H. J. Wang *et al.*, Nat. Commun. 4, 1940 (2013)], but also demonstrates the possibility to strongly polarize *weakly coupled* ^{13}C nuclei. This allows sensitive magnetic field control of the ^{13}C nuclear spin polarization for NMR applications and significant suppression of the ^{13}C nuclear spin noise to prolong the NV spin coherence time.

The atomic nuclear spins are central elements for NMR and magnetic resonance imaging[1] and promising candidates for storing and manipulating long-lived quantum information[2] due to their long coherence time. However, the tiny magnetic moment of the nuclear spins makes them completely random in thermal equilibrium, even in a strong magnetic field and at low temperature. This poses severe limitations on their applications. The dynamic nuclear polarization (DNP) technique can bypass this limitation by transferring the electron spin polarization to the nuclear spins via the hyperfine interaction (HFI), but efficient DNP is usually prohibited at room temperature.

An exception is the nitrogen-vacancy (NV) center[3] in diamond, which has an optically polarizable spin-1 electronic ground state with a long coherence time[4], allowing DNP at room temperature[5,6]. This prospect has attracted widespread interest due to its potential applications in room-temperature NMR, magnetic resonance imaging and magnetometry[7,8], electron-nuclear hybrid quantum register[9–11], and electron spin coherence protection by suppressing the nuclear spin noise[12]. In addition to the remarkable success in coherently driving spectrally resolved transitions to initialize, manipulate, and readout up to three strongly coupled nuclear spins[10,13–16], there are intense activities aiming to enhance the polarization of many nuclear spins via dissipative spin transfer from the NV to the nuclear spins. To overcome the large energy mismatch for resonant spin transfer, various strategies have been explored, e.g., tuning the NV spin near the excited state level anticrossing[6,17–22] or ground state level anticrossing (GSLAC)[5,23,24], driving the NV-nuclear spins into Hartman-Hahn resonance[25,26] or selectively driving certain spectrally resolved transitions between hyperfine-mixed states under optical illumination[27,28]. Successful polarization of bulk nuclear spins in diamond have dramatically enhanced the NMR signal by up to five orders of magnitudes[17,28] and significantly prolonged the NV spin coherence time[25,26]. In particular, near NV excited state level anticrossing, almost complete polarization has been achieved for the *on-site* ^{15}N (or ^{14}N) and the *strongly coupled* ^{13}C nuclei in the first shell of the vacancy[6,20–22,29].

Recently, Wang *et al.*[24] exploited the GSLAC to achieve near complete polarization of the strongly couled, first-shell ^{13}C nuclei and observed multiple reversals of the polarization direction over a narrow range (a few mT) of magnetic field. This interesting observation allows sensitive control of the polarization of *strongly coupled* ^{13}C nuclei by tuning the magnetic field, but a clear physical picture remains

[1]Hefei National Laboratory for Physical Sciences at the Microscale and Department of Modern Physics, University of Science and Technology of China, Hefei, Anhui 230026, China. [2]Beijing Computational Science Research Center, Beijing 100094, China. Correspondence and requests for materials should be addressed to W.Y. (email: wenyang@csrc.ac.cn)

absent. Furthermore, in most of the existing works, only a few *strongly coupled* nuclear spins (HFI $\gg$200 kHz) are significantly polarized via direct spin transfer from the NV center, while many weakly coupled nuclear spins are only slightly polarized via nuclear spin diffusion. Enhancing the polarization of these weakly coupled nuclear spins could further improve NMR and magnetic resonance imaging[17,27,28] and prolong the NV spin coherence time[25,26].

Motivated by the experimental observation of Wang *et al.*[24], in this paper we present an analytical formula for the DNP induced by an optically pumped NV center near the GSLAC at ambient temperature. It not only provides a clear physical picture for the experimentally observed polarization reversal of the *strongly coupled* ^{13}C nuclei (with HFI ~ 100 MHz) over a narrow range (a few mT) of magnetic field[24], but also reveals a simple strategy to (i) strongly polarize *weakly coupled* ^{13}C nuclei (with HFI down to ~kHz) and (ii) control the direction of their polarization by tuning the magnetic field over a much narrower range (~0.1 mT). First, we introduce an intuitive physical picture for our strategy. Then we present an analytical formula that substantiates this physical picture. Finally, we perform numerical simulations that demonstrate our strategy for a few hundred weakly coupled ^{13}C nuclei.

Results

Model and intuitive physical picture. Our model consists of a negatively charged NV center coupled to many surrounding nuclear spins at ambient temperature. The NV center has a ground state triplet $|\pm 1_g\rangle$ and $|0_g\rangle$ separated by zero-field splitting $D_{\rm gs} = 2.87$ GHz and an excited state triplet $|\pm 1_e\rangle$ and $|0_e\rangle$ separated by zero-field splitting $D_{\rm es} = 1.41$ GHz[29]. In a magnetic field B along the N-V axis (z axis), the electron Zeeman splitting $\gamma_e B$ cancels the ground state zero-field splitting at a critical magnetic field $B_{\rm LAC} \equiv D_{\rm gs}/\gamma_e \approx 102$ mT, leading to GSLAC between $|0_g\rangle$ and $|-1_g\rangle$. The GSLAC reduces the energy mismatch for the NV-nuclei flip flop and enables NV-induced DNP through their HFI $\sum_i \hat{\mathbf{F}}_i \cdot \hat{\mathbf{I}}_i$, where $\hat{\mathbf{F}}_i \equiv \hat{\mathbf{S}} \cdot \mathbf{A}_i$ and $\hat{\mathbf{S}}$ is the NV ground state spin.

Now we provide an intuitive physical picture for using an optically pumped NV center near the GSLAC to strongly polarize the nuclear spins and control their polarization direction by the magnetic field. For brevity we focus on one ^{13}C nuclear spin-1/2 and drop the nuclear spin index i. Since $|-1_g\rangle$ is nearly degenerate with the NV steady state $|0_g\rangle$ under optical pumping, the NV-nucleus flip flop is dominated by the nuclear spin raising transition $|0_g\rangle \otimes |\downarrow\rangle \rightarrow |-1_g\rangle \otimes |\uparrow\rangle$ and the nuclear spin lowering transition $|0_g\rangle \otimes |\uparrow\rangle \rightarrow |-1_g\rangle \otimes |\downarrow\rangle$, where $\{|\uparrow\rangle, |\downarrow\rangle\}$ are nuclear spin Zeeman eigenstates. The energy mismatch of the raising (lowering) transition is $\gamma_e(B_{\rm LAC} + \Delta_B/2 - B)$ [$\gamma_e(B_{\rm LAC} - \Delta_B/2 - B)$], where $\gamma_e(B_{\rm LAC} - B)$ is the $|-1_g\rangle - |0_g\rangle$ energy separation and $\Delta_B \equiv (2\gamma_N B - A_{zz})/\gamma_e$ comes from the nuclear Zeeman term $2\gamma_N B$ and the longitudinal HFI term $A_{zz} \equiv \mathbf{e}_z \cdot \mathbf{A} \cdot \mathbf{e}_z$. Since we always work near the GSLAC, where $2\gamma_N B/\gamma_e \approx 2\gamma_N B_{\rm LAC}/\gamma_e \approx 0.08$ mT, we can regard $\Delta_{\rm B}$ as a constant independent of the magnetic field B. The different energy mismatches make it possible to *selectively* drive one transition into resonance while keeping the other transition off resonance: set the magnetic field to $B_+ \equiv B_{\rm LAC} + \Delta_B/2$ ($B_- \equiv B_{\rm LAC} - \Delta_B/2$), so the raising (lowering) transition has a vanishing energy mismatch, i.e., on resonance, while the lowering (raising) transition has a finite energy mismatch $\gamma_e|\Delta_B|$, i.e., off resonance as long as the linewidth of the transition is smaller than $|\gamma_e \Delta_B|$. This highlights the linewidth (hereafter denoted by R) of the NV ground state as a crucial ingredient for achieving strong nuclear polarization: R/γ_e must be smaller than $|\Delta_B|$, so that the raising and the lowering transitions can be spectrally resolved. Below we show that the optical pumping is the dominant level-broadening mechanism, so that $R \propto$ optical pumping strength. Therefore, strong negative (positive) nuclear polarization can be achieved under sufficiently weak optical pumping ($R/\gamma_e \ll |\Delta_B|$) by tuning the magnetic field to B_- (B_+). The direction of the polarization can be reversed by switching the magnetic field between B_- and B_+. For first-shell ^{13}C nuclei, $|\Delta_B| \approx |A_{zz}|/\gamma_e \approx 5$ mT. This gives a simple explanation to the experimentally observed reversal of the polarization direction over a few mT[24]. For weakly coupled ^{13}C nuclei, $|\Delta_B| \approx 0.08$ mT, so the direction of the polarization can be reversed by sweeping the magnetic field over a much smaller range. Below we substantiate this physical picture with an analytical formula.

DNP theory of single nuclear spin. Under optical pumping, seven energy levels of the NV center are relevant (Fig. 1). The NV-nucleus coupled system obeys the Lindblad master equation

$$\dot{\hat{\rho}}(t) = \mathscr{L}_{\rm NV}\hat{\rho}(t) - i[\hat{H}_N + \hat{\mathbf{F}} \cdot \hat{\mathbf{I}}, \hat{\rho}(t)], \tag{1}$$

where $\mathscr{L}_{\rm NV}$ is the Liouville superoperator governing the NV evolution (including various dissipation processes as shown in Fig. 1) in the absence of the nuclear spin, $\hat{H}_N = \gamma_N B \hat{I}_z$ is the nuclear spin Zeeman Hamiltonian, and $\hat{\mathbf{F}} \cdot \hat{\mathbf{I}}$ is the NV-nucleus HFI. Equation (1) can be solved exactly by numerical simulation. However, this approach does not provide a clear physical picture, and it quickly becomes infeasible for multiple nuclear spins (to be discussed shortly), because the dimension of the Liouville space grows exponentially with the number of nuclei.

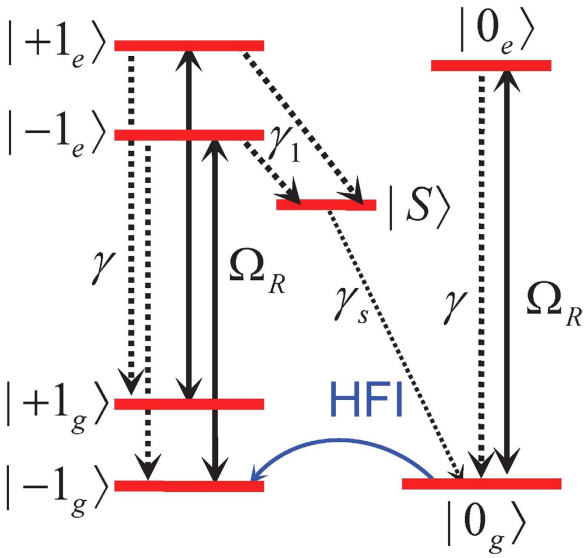

Figure 1. NV states at ambient temperature responsible for DNP under optical pumping.

Our work is based on a recently developed microscopic theory[30–32]. For the optically pumped NV center, this theory is applicable as long as the optical initialization time τ_c of the NV center is much shorter than the timescale of the DNP process, because in this case the NV center can be regarded as a non-equilibrium Markovian bath. Applying this theory to a ^{13}C nuclear spin-1/2, we obtain the rate equation $\dot{p}_\uparrow = -\dot{p}_\downarrow = -W_- p_\uparrow + W_+ p_\downarrow$ for the nuclear spin populations $p_\uparrow$ and $p_\downarrow$ $(=1 - p_\uparrow)$, where $W_+(W_-)$ is the rate of the nuclear spin raising (lowering) transition, as discussed in the previous subsection. The real-time evolution of the nuclear spin polarization $p \equiv p_\uparrow - p_\downarrow$ is given by $p(t) = p_{ss} + [p(0) - p_{ss}]e^{-Wt}$, where $p_{ss} \equiv (W_+ - W_-)/(W_+ + W_-)$ is the steady-state polarization and $W \equiv W_+ + W_-$ is the rate of DNP.

For weak optical pumping far from saturation, we can derive (see Methods) the following Fermi golden rule for the nuclear spin transition rates:

$$W_\pm = P_g 2\pi \left|\frac{A_{+\mp}}{2\sqrt{2}}\right|^2 \delta^{(R)}(\gamma_e(B_\pm - B)), \tag{2}$$

where $A_{+\mp} \equiv \mathbf{e}_+ \cdot \mathbf{A} \cdot \mathbf{e}_\mp$ with $\mathbf{e}_\pm \equiv \mathbf{e}_x \pm i\mathbf{e}_y$, $P_g = (R + \gamma)/(2R + \gamma)$ is the steady-state population of the NV center on $|0_g\rangle$, $\delta^{(R)}(x) \equiv (R/\pi)/(x^2 + R^2)$ is the Lorentzian shape function, and the optically induced NV ground state level broadening R *is equal to the optical pumping rate*, i.e., the number of optical transitions per unit time from the NV ground orbital to the excited orbital (see Methods). This optically induced level broadening is typically much larger than the intrinsic NV spin decoherence rate (~1 kHz) and provides a microscopic explanation for the previously observed NV level broadening under laser illumination[23,33]. Most importantly, Eq. (2) quantifies the physical picture discussed in the previous subsection: to achive strong negative (positive) nuclear polarization, we can use weak optical pumping $(R/\gamma_e \ll |\Delta_B|)$ and set the magnetic field to B_- (B_+), so that the rate W_- (W_+) of the nuclear spin lowering (raising) transition is resonantly enhanced, while the rate W_+ (W_-) of the nuclear spin raising (lowering) transition is suppressed. The relation $W_\pm \propto |A_{+\mp}|^2$ also suggests that the polarization p_{ss} depends strongly on the HFI tensor $\mathbf{A}$, e.g., for the ^{15}N nucleus with $A_{xx} = A_{yy}$ and $A_{xy} = 0$, we have $A_{++} = 0$ and $A_{+-} = 2A_{xx}$, and hence $p_{ss} \approx 100\%$.

Equation (2) is accurate only when the DNP time $1/W$ calculated from Eq. (2) $\gg$ NV optical initialization time $\tau_c \approx ([R\gamma_1/(\gamma_1 + \gamma)]^{-1} + \gamma_s^{-1})$, so that the NV center is a Markovian bath. When the optical pumping rate R is so small or the HFI is so strong that the DNP time calculated from Eq. (2) drops below τ_c, the NV center becomes a non-Markovian bath and Eq. (2) becomes inaccurate, e.g., instead of dropping below τ_c, the true DNP time would be lower bounded by $\sim\tau_c$. This can be easily understood: since the nuclear spin dissipation originates from the dissipation of the optically pumped NV center, the timescale $1/W$ of the nuclear spin dissipation should be longer than the time sclae τ_c of the NV center dissipation.

Up to now, we have neglected other nuclear spin relaxation mechanisms, such as spin-lattice relaxation and HFI with NV excited states. The former occurs on the time scale ranging from a few seconds to tens of minutes[17,34]. The latter can be estimated from the Fermi golden rule, e.g., for a ^{13}C located at

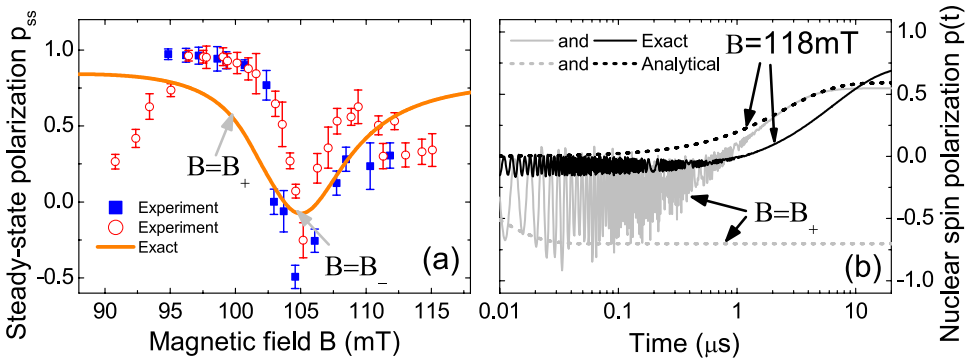

Figure 2. (**a**) p_{ss} of a first-shell ^{13}C nucleus: exact numerical solution to Eq. (1) (orange solid line) compared with the experimentally deduced nuclear polarization[24] (filled squares and empty circles) from two different analysis methods. (**b**) Real-time evolution of nuclear polarization $p(t)$ at B_+ or far from B_+: exact solution to Eq. (1) vs. our analytical formula Eq. (7).

3Å away from the NV center, the dipolar HFI gives a nuclear spin relaxation time >1 s. These effects are described by nuclear depolarization $W_\pm \to W_\pm + \gamma_{dep}$, which increases W by $2\gamma_{dep}$ and decreases p_{ss} by a factor $1 + 2\gamma_{dep}/W$, i.e., nuclear depolarization is negligible when $W \gg 2\gamma_{dep}$.

Below we first specialize to strongly coupled ^{13}C nuclei, where $W \gg 2\gamma_{dep}$ is always satisfied, so the nuclear depolarization is negligible. Then we consider weakly coupled ^{13}C nuclei, where $W \gg 2\gamma_{dep}$ becomes a crucial condition for achieving strong nuclear polarization. In all our calculations, we use the experimentally measured parameters at room temperature (cf. Fig. 1): excited state orbital pure dephasing $\Gamma_e = 10^4$GHz[35], radiative decay rate $\gamma = 13$ MHz[36], and intersystem crossing rates $\gamma_1 \approx 13.3$ MHz[37] and $\gamma_s = 0.56$ MHz[38–41]. Unless explicitly mentioned, the very small leakage from $|0_e\rangle$ to $|\pm 1_g\rangle$ is neglected, consistent with the experimentally reported[14,42] high optical initialization probability ~96% into $|0_g\rangle$. The effect of imperfect NV optical initialization will be discussed shortly.

DNP of strongly coupled ^{13}C nucleus. To begin with, we consider the DNP of a *strongly coupled* ^{13}C nucleus in the first shell of the NV center under optical pumping near the $|0_g\rangle$–$|-1_g\rangle$ GSLAC. This configuration has been studied experimentally in ensembles of NV centers[24], which shows a reversal of the direction of the ^{13}C nuclear polarization over a narrow range (~a few mT) of magnetic fields. This interesting observation allows sensitive control of the polarization of the strongly coupled ^{13}C nuclei by tuning the magnetic field, but a clear physical picture remains absent. Here the very strong HFI makes the DNP time calculated from Eq. (2) much shorter than τ_c, so our analytical formula are not accurate. In this case, we numerically solve Eq. (1) using the experimentally measured ground state HFI tensor[19,24,43,44] with nonzero components $A_{xx} = 198.6$ MHz, $A_{yy} = 123.0$ MHz, $A_{zz} = 129.0$ MHz and $A_{xz} = A_{zx} = -21.5$ MHz. To focus on the intrinsic behavior of the DNP, we set $\gamma_{dep} = 0$. We have verified that due to the strong HFI induced NV-^{13}C mixing, the ^{13}C nuclear polarization depends weakly on the optical pumping up to $R < 4$ MHz. In our numerical calculation, we take $R = 0.4$ MHz.

In Fig. 2(a), the numerically calculated nuclear polarization (black solid line) correctly reproduces the sign reversal of the experimentally deduced nuclear polarization[24] (circles and squares). Actually, although our analytical formula in Eq. (2) is not accurate, it still provides a clear physical picture for the polarization reversal: the negative polarization dip in Fig. 2(a) originates from the resonance of the nuclear spin lowering transition at $B_- \approx 105$ mT, while the positive polarization away from B_- originates from the dominance of the raising transition rate $W_+ \propto |A_{+-}|^2$ over the lowering transition rate $W_- \propto |A_{++}|^2$ since $|A_{+-}| \approx 322$ MHz is significantly larger than $|A_{++}| \approx 76$ MHz. We notice that there is significant difference between our numerical results and the experimentally deduced nuclear polarization from the ODMR spectrum, especially in the magnitude of the negative dip. We tentatively attribute this discrepancy to two factors. First, all the parameters used in our calculation are taken from previous experimental measurements and/or first-principle calculations, which may differ from the particular experiment of Wang *et al.*[24]. Second, the estimate of the nuclear polarization from the ODMR spectrum involves a series of assumptions such as the lack of quantum coherence between different NV-^{13}C mixed levels, so the uncertainty of this estimate is relatively large, e.g., the estimates based on different transitions give different results, denoted by the circles and squares in Fig. 2(a).

For the first-shell ^{13}C nucleus[24], the NV center is not a Markovian bath and the numerically calculated nuclear polarization [solid lines in Fig. 2(b)] exhibit strong non-Markovian oscillation. In this regime, our analytical results [dashed lines in 2(b)] are not valid. However, as long as the DNP time $1/W$ calculated from Eq. (2) is much longer than τ_c, e.g., for weakly coupled ^{13}C nuclei, our analytical formula

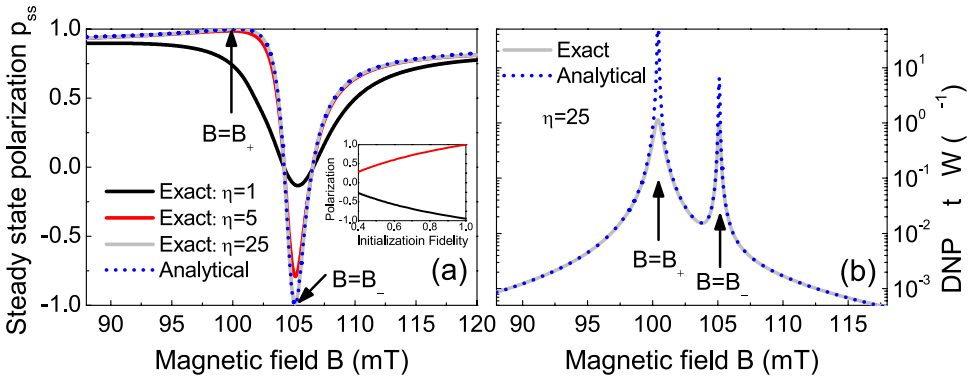

Figure 3. (**a**) Steady-state polarization p_{ss} of a first-shell ^{13}C nucleus: exact numerical solution to Eq. (1) (solid lines) vs. analytical formula Eq. (2) (dotted line). To illustrate the convergence of our theory, we set $A_{xz} = A_{zx} = 0$ and reduce A_{xx} and A_{yy} by a factor $\eta = 1$ (black line), 5 (red line), and 25 (gray line). (**b**) DNP rate for $\eta = 25$: exact solution to Eq. (1) (gray solid line) vs. analytical formula Eq. (2) (blue dotted line).

becomes accurate. To demonstrate this point, we keep A_{zz} invariant, set $A_{xz} = A_{zx} = 0$, and reduce A_{xx} and A_{yy} by a factor η (i.e., $A_{xx} \to A_{xx}/\eta$ and $A_{yy} \to A_{yy}/\eta$), so that the nuclear spin transition rates $W_{\pm} \propto |A_{+\mp}|^2$ are reduced by a factor η^2. In Fig. 3(a), the agreement between the analytical results and the exact numerical results improves successively with increasing η, e.g., excellent agreement is reached for $\eta = 125$. In Fig. 3(b), when the magnetic field approaches $B_{\pm}$ (i.e., resonance of the raising or lowering transition), the DNP rate calculated from Eq. (2) sharply peaks and significantly exceeds $1/\tau_c \approx (1.1\ \mu s)^{-1}$, while the exact numerical result saturates to ~$(1.6\mu s)^{-1}$. Away from $B_{\pm}$, our analytical DNP rate $\ll 1/\tau_c$ and hence agrees well with the exact result.

DNP of weakly coupled ^{13}C nucleus. An important feature in Fig. 2(a) is that when the HFI decreases, the positive (negative) polarization peak (dip) at B_+ (B_-) approaches +100% (−100%) due to the resonance of the nuclear spin raising (lowering) transition. This indicates the possibility of achieving strong positive (negative) nuclear polarization for weakly coupled nuclear spins by tuning the magnetic field to B_+ (B_-). In the above calculations, we have assumed perfect optical initialization of the NV center into $|0_g\rangle$ by neglecting the small intersystem crossing from $|0_e\rangle$ to $|\pm 1_g\rangle$. Actually, strong nuclear polarization can be achieved even when the NV initialization is not perfect: as shown in the inset of Fig. 3(a), the maximal nuclear polarization at $B_{\pm}$ only decreases sublinearly with increasing initialization error, e.g., the nuclear polarization remains slightly above 80% when the optical initialization fidelity decrease to 80%. Since the nuclear polarization is not so sensitive to the NV optical initialization fidelity, hereafter we always assume perfect optical initialization of the NV center.

Now based on the analytical formula in Eq. (2), we discuss in detail the conditions for strongly polarizing distant ^{13}C nuclei with weak HFI ($|A_{zz}| \ll |2\gamma_N B_{LAC}|$), so that the separation between B_+ and B_- is $|\Delta_B| \approx |2\gamma_N B_{LAC}|/\gamma_e \approx 0.08$ mT. Since we need to tune the magnetic field to B_+ or B_-, the experimental control precision δB of the magnetic field should be smaller than 0.08 mT. This is accessible by current experimental techniques, e.g., $\delta B = 0.002$ mT has been reported[34]. Another obvious condition is that the nuclear depolarization, which always tends to decrease the nuclear polarization, should be negligible, i.e., the maximal DNP rate $\gtrsim 2\gamma_{dep}$ or equivalently $|A_{++}|^2 + |A_{+-}|^2 \gg 4R\gamma_{dep}$. This requires that the HFI should not be too weak, e.g., for $R = 0.2$ MHz and $\gamma_{dep} = 1\ s^{-1}$, this requires the HFI to be larger than 1 kHz. Hereafter we assume that this condition is satisfied. The intuitive physical picture suggests that the linewidth R (=optical pumping rate) of the NV ground state is essential, so we divide our following discussion into strong optical pumping and weak optical pumping, respectively.

Under strong optical pumping ($R/\gamma_e > |\Delta_B| \approx 0.08$ mT), the resonances at $B_{\pm}$ are not spectrally resolved. In this case, the nuclear polarization is uniquely determined by the HFI tensor **A**. For dipolar HFI,

$$p_{ss} \approx \frac{2}{c_\theta + 1/c_\theta} \tag{3}$$

is uniquely determined by the polar angle θ of the ^{13}C location **R** through $c_\theta \equiv 3\cos^2\theta - 2$. For example, in Fig. 4(c), the resonance of the nuclear spin raising transition at $B_+ \approx 102.37$ mT (marked by white dotted lines) and the resonance of the nuclear spin lowering transition at $B_- \approx 102.45$ mT (marked by black dotted lines) are significantly broadened along the magnetic field axis and are not clearly resolved.

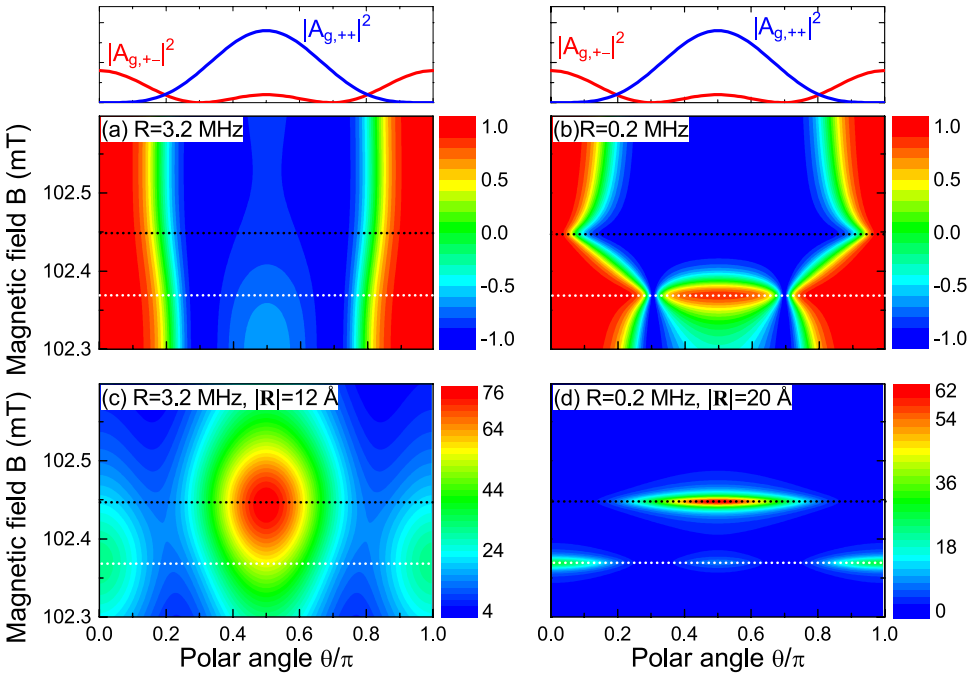

Figure 4. Steady state nuclear polarization p_{ss} [(**a**) and (**b**)] and DNP rate W in units of Hz [(**c**) and (**d**)] by dipolar HFI with the NV center, calculated from the analytical formula Eq. (2) with optical pumping rates $R = 3.2$ MHz [(**a**) and (**c**)] and 0.2 MHz [(**b**) and (**d**)].The distance of the ^{13}C nucleus from the NV center is $|\mathbf{R}| = 12$ Å in (c) and $|\mathbf{R}| = 20$ Å in (d). The white (black) dotted line indicates the magnetic field B_+ (B_-).

The most interesting case is weak optical pumping ($R/\gamma_e < |\Delta_B| \approx 0.08$ mT), where the nuclear spin raising and lowering transitions are spectrally resolved and can be selectively driven into resonance to achieve strong positive (negative) nuclear polarization by tuning the magnetic field to B_+ (B_-). For example, in Fig. 4(d), the very narrow resonance peak of the raising transition at B_+ (marked by white dotted lines) and the resonance peak of the lowering transition at B_- (marked by black dotted lines) are clearly resolved. Correspondingly, in Fig. 4(b), these resonances give rise to strong positive (negative) nuclear polarization near B_+ (B_-), superimposed on the usual dependence on the polar angle θ via $W_\pm \propto |A_{+\mp}|^2 \propto (1 \pm c_\theta)^2$ [plotted on top of Figs 4(a),(b)]. We notice that a ^{13}C nucleus located at $|\mathbf{R}| = 20$ Å away from the NV center can be highly polarized at a rate ~60 Hz = (2.6 ms)$^{-1}$, sufficient to overcome the slow nuclear depolarization $\gamma_{dep} \sim 1\,s^{-1}$.

DNP of multiple ^{13}C nuclei. Having established a complete picture for single-^{13}C DNP, now we generalize the above results to many ($N \gg 1$) ^{13}C nuclear spins coupled to the NV center via $\hat{H}_{HF} = \sum_{i=1}^{N} \hat{\mathbf{F}}_i \cdot \hat{\mathbf{I}}_i$, where $\hat{\mathbf{F}}_i = \hat{\mathbf{S}} \cdot \mathbf{A}_i$ and the excited state HFI is neglected because the induced NV-nuclei flip-flop processes are off-resonant. In the same spirit as that in treating the DNP of a single nuclear spin, we decompose the HFI into the longitudinal part $\sum_{i=1}^{N} \hat{F}_{i,z}\hat{I}_{i,z}$ and the transverse part $\sum_{i=1}^{N}(\hat{F}_{i,+}\hat{I}_{i,-} + h.c.)/2$. Then we approximate the longitudinal part with $-|-1_g\rangle\langle -1_g|\hat{h}_z$ (which is treated *exactly*) and treat the transverse HFI with second-order perturbation theory, where

$$\hat{h}_z \equiv \sum_{i=1}^{N} A_{i,zz}\hat{I}_{i,z} \tag{4}$$

is the collective Overhauser field from all the nuclei.

The physical picture of the many-nuclei DNP is as follows. Up to leading order, the flip of different nuclei by the transverse HFI is independent, in the sense that at a given moment, only one nuclear spin is being flipped, while other nuclear spins simply act as " spectators" . However, the flip of each individual nuclear spin does depend on the states of all the nuclear spins via the collective Overhauser field $\hat{h}_z$: each many-nuclei state $|\mathbf{m}\rangle = \otimes_{i=1}^{N} |m_i\rangle$ ($|m_i\rangle$ is the Zeeman eigenstate of the ith nucleus) produces an Overhauser field $h_\mathbf{m} \equiv \langle \mathbf{m}|\hat{h}_z|\mathbf{m}\rangle$ that shifts the energy of the NV state $|-1_g\rangle$ by an amount $-h_\mathbf{m}$. This renormalizes the $|-1_g\rangle$–$|0_g\rangle$ separation from $\gamma_e(B_{LAC} - B)$ to $\gamma_e(B_{LAC} - B) - h_\mathbf{m}$ and hence changes the NV dynamics and NV-induced nuclear spin flip, e.g., the raising and lowering transition rates

$W_{i,\pm}(h_{\mathbf{m}})$ of the ith nucleus conditioned on the many-nuclei state being $|\mathbf{m}\rangle$ is obtained from Eq. (2) by replacing $\mathbf{A}$, B with $\mathbf{A}_i$, $B + h_{\mathbf{m}}/\gamma_e$, respectively.

The above physical picture is quantified by the following rate equations for the diagonal elements $p_{\mathbf{m}} \equiv \langle \mathbf{m}|\hat{p}|\mathbf{m}\rangle$ of the many-nuclei density matrix $\hat{p}$:

$$\begin{aligned}\dot{p}_{\mathbf{m}} = &-\sum_i \Big[W_{i,+}(h_{\mathbf{m}})p_{\mathbf{m}} - W_{i,-}\big(h_{\mathbf{m}+1_i}\big)p_{\mathbf{m}+1_i}\Big] \\ &-\sum_i \Big[W_{i,-}(h_{\mathbf{m}})p_{\mathbf{m}} - W_{i,+}\big(h_{\mathbf{m}-1_i}\big)p_{\mathbf{m}-1_i}\Big],\end{aligned} \tag{5}$$

which has been derived by adiabatically decoupling the fast electron dynamics from the slow DNP process[30–32]. Here $|\mathbf{m} + 1_i\rangle = \hat{I}_i^+|\mathbf{m}\rangle$ is the same as $|\mathbf{m}\rangle$ except that the state of the ith nucleus changes from $|m_i\rangle$ to $|m_i + 1\rangle$. Now we discuss the difference between single-spin DNP and many-spin DNP. In the latter case, the DNP of each individual nucleus occurs in the presence of many " spectator" nuclei, which produce a fluctuating Overhauser field $\hat{h}_z$ that randomly shifts the NV energy levels, such that the $|-1_g\rangle$-$|0_g\rangle$ separation changes from $\gamma_e(B_{\mathrm{LAC}} - B)$ to a random value $\gamma_e(B_{\mathrm{LAC}} - B) - \hat{h}_z$. The effect of the Overhauser field is equivalent to a random magnetic field $\hat{h}_z/\gamma_e$ on the NV center, which makes it more difficult to tune the external magnetic field to match the resonance of the nuclear spin raising and lowering transitions. More precisely, a finite mismatch $\sim (h_z)_{\mathrm{rms}}$ makes the originally resonant raising (lowering) transition off-resonant, and hence reduce the resonant DNP rate by a factor $(h_z)_{\mathrm{rms}}^2/R^2$. For example, a natural abundance of ^{13}C nuclei gives a typical Overhauser field $(h_z)_{\mathrm{rms}} \sim 0.2$ MHz. This reduces the typical DNP rate by a factor of 2 for the optical pumping rate $R = 0.2$ MHz, e.g., the maximal DNP rate ~60 Hz [Fig. 4(d)] for a ^{13}C nucleus at 2 nm away from the NV center is reduced to 30 Hz $\approx (5\ \mathrm{ms})^{-1}$, which is still sufficient to overcome the slow nuclear depolarization $\gamma_{\mathrm{dep}} \sim 1\,\mathrm{s}^{-1}$. Therefore, under weak pumping $R/\gamma_e \ll |\Delta_B|$, the typical Overhauser field fluctuation $(h_z)_{\mathrm{rms}} \ll |\gamma_e \Delta_B|$ does not significantly influence the nuclear polarization.

For N nuclear spin-1/2's, the number of variables $\{p_{\mathbf{m}}\}$ is 2^N. When N is small, we can solve Eq. (5) exactly. For large N, however, the exponentially growing complexity prohibit an exact solution to Eq. (5). Here, we introduce a mean-field method (see Methods). It provides a good approximation to the average polarization $\overline{p}_{\mathrm{ss}} = (1/N)\sum_{i=1}^{N} p_{i,\mathrm{ss}}$ and average Overhauser field $h_{\mathrm{ss}} = \sum_i A_{i,zz} p_{i,\mathrm{ss}}/2$, but does not include any spin-spin correlation effect, such as feedback induced spin bath narrowing[12,30–32,45–48].

As shown in Fig. 5(a), for a small number ($N = 7$) of randomly chosen ^{13}C nuclei coupled to the NV via dipolar HFI, the average polarization $\overline{p}_{\mathrm{ss}}$ from the mean-field approximation agrees well with the exact solution to Eq. (5). For $N = 400$ randomly chosen ^{13}C nuclei, the exact solution is no longer available and we plot the approximation results in Fig. 5(b). Both Figs 5(a),(b) clearly demonstrate that with decreasing optical pumping rate, the nuclear polarization shows a successively stronger peak (dip) at the resonant magnetic field $B_+ \approx 102.37$ mT ($B_- \approx 102.45$ mT). The relatively stronger polarization at B_- arises from the dependence $W_{\mp} \propto |A_{+\mp}|^2 \propto (1 \pm c_\theta)^2$ on the polar angle θ of the nuclear spin location: more nuclear spins have $|A_{++}|^2 > |A_{+-}|^2$ [as plotted on top of Figs 4(a),(b)] and hence favors negative polarization. These results clearly demonstrate the possibility to strongly polarize weakly coupled ^{13}C nuclear spins by using weak optical pumping near $B_\pm$. The polarization of these weakly coupled ^{13}C nuclei is ultimately limited by nuclear depolarization, which becomes significant when the HFI becomes too weak. This can be clearly seen in the spatial distribution of the nuclear polarization near B_+ [Fig. 5(c)] and B_- [Fig. 5(d)]. Near B_+, strong positive polarization is achieved for ^{13}C nuclei with $|\mathbf{R}| < 15$ Å away from the NV center, corresponding to dipolar HFI strength > 6 kHz. For more distant ^{13}C nuclei, the HFI strength is too weak for the DNP to dominate over the nuclear depolarization, so their polarization drops significantly. Similarly, near B_-, strong negative polarization can be achieved for ^{13}C nuclei with $|\mathbf{R}| < 25$ Å away from the NV center, corresponding to dipolar HFI strength ~1 kHz.

Finally, we recall that the on-site ^{15}N or ^{14}N nucleus has an isotropic transverse HFI and hence $W_- = |A_{++}|^2 = 0$, i.e., they could be completely polarized and thus does not significantly influence the DNP of the ^{13}C nuclei, except for a shift of the $|-1_g\rangle$-$|0_g\rangle$ separation by ~2.2 MHz (for ^{14}N) or ~3 MHz (for ^{15}N), corresponding to a shift of the resonance magnetic field by ~0.78 G (for ^{14}N) or ~1.1 G (for ^{15}N).

Discussion

In conclusion, we have presented a comprehensive theoretical understanding on the dynamic nuclear polarization induced by an optically pumped NV center near the ground state anticrossing at ambient temperature. Our results not only provide a clearly physical picture for a recently observed[24] magnetic field dependence of the polarization direction of first-shell ^{13}C nuclei, but also reveals an efficient scheme to strongly polarize weakly coupled ^{13}C nuclear spins ~25 Å away from the NV center (HFI strength ~1 kHz) by tuning the magnetic field under weak optical pumping. These results provide a clear guidance for optimizing future dynamic nuclear polarization experiments. For example, this scheme could be used

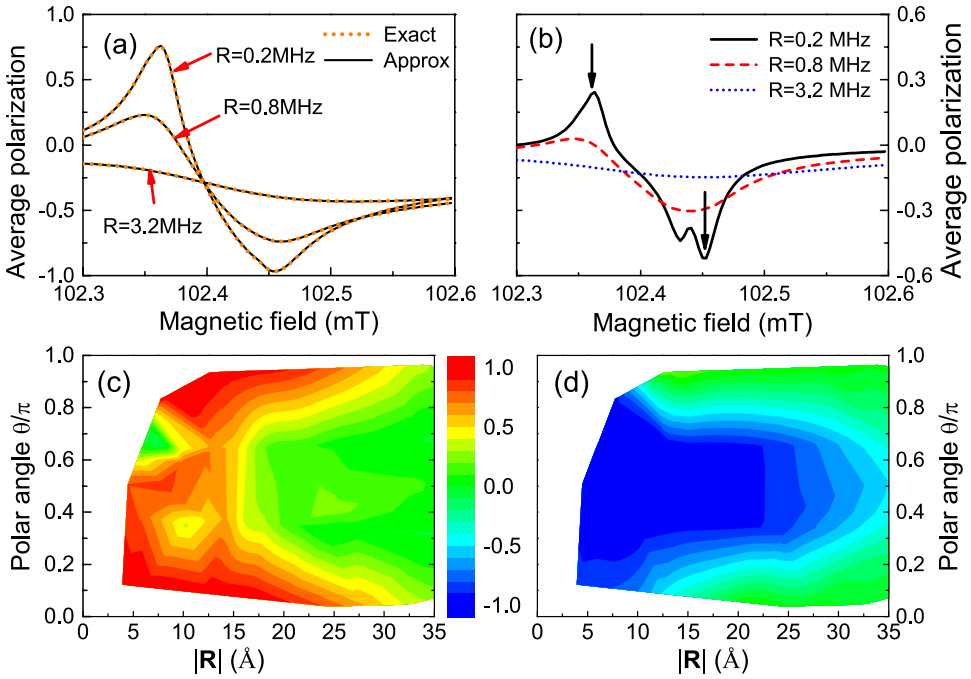

Figure 5. Average polarization $\overline{p}_{ss}$ of (**a**) N = 7 and (**b**) $N = 400$ randomly chosen ^{13}C nuclei for different optical pumping rates $R =$ 0.2, 0.8, and 3.2 MHz**.** For $R = 0.2$ MHz, the spatial distribution of the polarization of $N = 400$ randomly chosen ^{13}C nuclei in a magnetic field (c) 102.36 mT and (d) 102.45 mT [marked by the arrows in panel (b)]. The depolarization rate $\gamma_{dep} = 1$ Hz for all panels.

to polarize distant ^{13}C nuclei in isotope purified diamond[4] to further prolong the NV coherence time. An important limitation of our method is that it requires good alignment of the magnetic field along the N-V axis, because a tilted magnetic field would dramatically decrease the population on $|0_g\rangle$ and hence degrade the nuclear polarization. For nanodiamonds containing a single NV center, we need to first align this NV center to the magnetic field before using this NV center to polarize weakly coupled ^{13}C nuclear spins.

Methods

Derivation of nuclear spin transition rates. According to the theory[30–32], the populations $\{p_m\}$ of a single nuclear spin-I on its Zeeman sublevels $|m\rangle$ $(m = -I, -I+1, \cdots, I)$ obey the rate equations

$$\dot{p}_m = \sum_{n=m\pm1} W_{m\leftarrow n} p_n - \left(\sum_{n=m\pm1} W_{n\leftarrow m}\right) p_m. \tag{6}$$

Up to second order of the *tranvserse* HFI $(\hat{F}_+\hat{I}_- + \hat{F}_-\hat{I}_+)/2$ (longitudinal HFI $F_z I_z$ treated *exactly*), the transition rate from $|m\rangle$ to $|m \pm 1\rangle$ is[32]

$$W_{m\pm1\leftarrow m} = \frac{\xi_m^{\pm}}{2}\,\mathrm{Re}\int_0^{+\infty} dt\; e^{\mp i\gamma_N B t}\,\mathrm{Tr}_{\mathrm{NV}}\hat{F}_{\mp}^{\dagger} e^{\mathcal{L}_{m\pm1,m}t}\hat{F}_{\mp}\hat{P}_m, \tag{7}$$

where $\xi_m^{\pm} \equiv \langle m|\hat{I}_{\mp}\hat{I}_{\pm}|m\rangle$, the Liouville superoperator $\mathscr{L}_{n,m}(\bullet) \equiv \mathscr{L}_{\mathrm{NV}}(\bullet) - i[n\hat{F}_z(\bullet) - (\bullet)m\hat{F}_z]$, and $\hat{P}_m$ is the NV steady state in the rotating frame conditioned on the nuclear spin state being $|m\rangle$, i.e., $\mathscr{L}_{m,m}\hat{P}_m = 0$ and $\mathrm{Tr}_{\mathrm{NV}}\hat{P}_m = 1$.

Since we consider the NV center near the GSLAC, we can exclude the energy levels $|+1_g\rangle$ and $|+1_e\rangle$, which have vanishingly small occupation. Under this approximation, the rotating frame Hamiltonian of the five-level NV model is

$$\hat{H}_{\mathrm{NV}} = \left(D_{gs} - \gamma_e B\right)\hat{\sigma}_{-1_g,-1_g} + \left(D_{\mathrm{es}} - \gamma_e B + \omega_0 - \omega\right)\hat{\sigma}_{-1_e,-1_e} + \frac{\Omega_R}{2}\left(\hat{\sigma}_{-1_e,-1_g} + h.\,c.\right), \tag{8}$$

where $\hat{\sigma}_{ij} \equiv |i\rangle\langle j|$. Neglecting $\hat{F}_z$-induced NV spin mixing, the longitudinal HFI reduces to $-A_{zz}\hat{\sigma}_{-1_g,-1_g}\hat{I}_z$. Neglecting the non-collinear term $\propto \hat{S}_z\hat{I}_\pm$ (as the NV mostly stays in $|0_g\rangle$) and the NV excited state HFI (which is far off-resonant), the transverse HFI reduces to $(\hat{F}_+\hat{I}_- + h.\,c.)/2$ with

$\hat{F}_+ = (\hat{\sigma}_{-1_g,0_g}A_{++} + \hat{\sigma}_{0_g,-1_g}A_{-+})/\sqrt{2}$. To calculate $W_{m\pm1\leftarrow m}$ from Eq. (7), we first determine the NV steady state as $\hat{P}_{m,m} = P_g\hat{\sigma}_{0_g,0_g} + (1-P_g)\hat{\sigma}_{0_e,0_e}$, where $R = 2\pi(\Omega_R/2)^2\delta^{((\gamma+\Gamma_e+\gamma_\varphi)/2)}(\omega_0-\omega)$ is the optical pumping rate for $|0_g\rangle \leftrightarrow |0_e\rangle$. Substituting into Eq. (7) gives

$$W_{m\pm1\leftarrow m} = -\xi_m^{\pm}\frac{|A_{+\mp}|^2}{4}P_g\,\mathrm{Re}\,\rho^{\pm}_{-1_g,0_g}, \tag{9}$$

where $\rho^{(\pm)}_{i,j} \equiv \langle i|\hat{\rho}^{(\pm)}|j\rangle$ is the (i,j) matrix element of the operator $\hat{\rho}^{(\pm)} \equiv (\mathscr{L}_{m\pm1,m} \mp \gamma_N B)^{-1}\hat{\sigma}_{-1_g,0_g}$, which is a linear combination of $\hat{\sigma}_{-1_g,0_g}$, $\hat{\sigma}_{-1_e,0_g}$, $\hat{\sigma}_{-1_g,0_e}$, and $\hat{\sigma}_{-1_e,0_e}$.

Now we calculate $\rho^{(\pm)}_{-1_g,0_g}$ by taking the $\langle 0_g|\bullet|-1_g\rangle$, $\langle -1_e|\bullet|0_g\rangle$, $\langle -1_g|\bullet|0_e\rangle$ and $\langle -1_e|\bullet|0_e\rangle$ matrix elements of

$$(\mathscr{L}_{m\pm1,m} \mp \gamma_N B)\hat{\rho}^{(\pm)} = \hat{\sigma}_{-1_g,0_g}, \tag{10}$$

which gives four coupled equations

$$\begin{aligned}
&\left(\Delta^{(\pm)}_{-1_g,0_g} - i\Gamma_{-1_g,0_g}\right)\rho^{(\pm)}_{-1_g,0_g} + \frac{\Omega_R}{2}\left(\rho^{(\pm)}_{-1_e,0_g} - \rho^{(\pm)}_{-1_g,0_e}\right) = i,\\
&\left(\Delta^{(\pm)}_{-1_e,0_g} - i\Gamma_{-1_e,0_g}\right)\rho^{(\pm)}_{-1_e,0_g} + \frac{\Omega_R}{2}\left(\rho^{(\pm)}_{-1_g,0_g} - \rho^{(\pm)}_{-1_e,0_e}\right) = 0,\\
&\left(\Delta^{(\pm)}_{-1_g,0_e} - i\Gamma_{-1_g,0_e}\right)\rho^{(\pm)}_{-1_g,0_e} - \frac{\Omega_R}{2}\left(\rho^{(\pm)}_{-1_g,0_g} - \rho^{(\pm)}_{-1_e,0_e}\right) = 0,\\
&\left(\Delta^{(\pm)}_{-1_e,0_e} - i\Gamma_{-1_e,0_e}\right)\rho^{(\pm)}_{-1_e,0_e} - \frac{\Omega_R}{2}\left(\rho^{(\pm)}_{-1_e,0_g} - \rho^{(\pm)}_{-1_g,0_e}\right) = 0.
\end{aligned} \tag{11}$$

Here $\Delta^{(\pm)}_{j,i}$ is the energy difference between $|j\rangle|m\pm1\rangle$ and $|i\rangle|m\rangle$ ($|i\rangle$, $|j\rangle$ are NV states and $|m\rangle$, $|m\pm1\rangle$ are nuclear Zeeman states), i.e.,

$$\begin{aligned}
\Delta^{(\pm)}_{-1_g,0_g} &= D_{\mathrm{gs}} - \gamma_e B \pm \gamma_N B - (m\pm1)A_{zz},\\
\Delta^{(\pm)}_{-1_e,0_e} &= D_{\mathrm{es}} - \gamma_e B \pm \gamma_N B,\\
\Delta^{(\pm)}_{-1_e,0_g} &= E^{(\pm)}_{-1_e,0_e} + \omega_0 - \omega,\\
\Delta^{(\pm)}_{-1_g,0_e} &= E^{(\pm)}_{-1_g,0_g} - \omega_0 + \omega,
\end{aligned} \tag{12}$$

and $\Gamma_{j,i}$ is the linewidth of the NV transition $|i\rangle \leftrightarrow |j\rangle$, i.e., $\Gamma_{-1_g,0_g} = \gamma_\varphi$, $\Gamma_{-1_e,0_e} = \gamma + \gamma_1/2$, $\Gamma_{-1_e,0_g} = (\Gamma_e + \gamma + \gamma_1 + \gamma_\varphi)/2$, and $\Gamma_{-1_g,0_e} = (\Gamma_e + \gamma + \gamma_\varphi)/2$. Eliminating $\rho^{(\pm)}_{-1_e,0_g}$ and $\rho^{(\pm)}_{-1_g,0_e}$ gives the " rate equations":

$$\begin{aligned}
&\left(\Delta^{(\pm)}_{-1_g,0_g} - i\Gamma_{-1_g,0_g} - \mathscr{R}^{(\pm)}\right)\rho^{(\pm)}_{-1_g,0_g} + \mathscr{R}^{(\pm)}\rho^{(\pm)}_{-1_e,0_e} = i,\\
&\left(\Delta^{(\pm)}_{-1_e,0_e} - i\Gamma_{-1_e,0_e} - \mathscr{R}^{(\pm)}\right)\rho^{(\pm)}_{-1_e,0_e} + \mathscr{R}^{(\pm)}\rho^{(\pm)}_{-1_g,0_g} = 0,
\end{aligned} \tag{13}$$

from which we obtain the solution

$$\rho^{(\pm)}_{-1_g,0_g} = \frac{i}{\Delta^{(\pm)}_{-1_g,0_g} - i\Gamma_{-1_g,0_g} - \mathscr{R}^{(\pm)}\left(1 + \frac{\mathscr{R}^{(\pm)}}{\Delta^{(\pm)}_{-1_e,0_e} - i\Gamma_{-1_e,0_e} - \mathscr{R}^{(\pm)}}\right)}, \tag{14}$$

where $\mathscr{R}^{(\pm)} = \mathscr{R}^{(\pm)}_0 + \mathscr{R}^{(\pm)}_{-1}$ with $\mathscr{R}^{(\pm)}_0 \equiv (\Omega_R/2)^2/(\Delta^{(\pm)}_{-1_g,0_e} - i\Gamma_{-1_g,0_e})$ and $\mathcal{R}^{(\pm)}_{-1} \equiv (\Omega_R/2)^2/\left(\Delta^{(\pm)}_{-1_e,0_g} - i\Gamma_{-1_e,0_g}\right)$the *complex* self-energy corrections to $|0_g\rangle$ and $|-1_g\rangle$ by the optical pumping $|0_g\rangle \leftrightarrow |0_e\rangle$ and $|-1_g\rangle \leftrightarrow |-1_e\rangle$, respectively. More precisely, the optical pumping $|0_g\rangle \leftrightarrow |0_e\rangle$ ($|-1_g\rangle \leftrightarrow |-1_e\rangle$) induces an optical Stark shift $\mathrm{Re}\,\mathscr{R}^{(\pm)}_0$ ($-\mathrm{Re}\,\mathscr{R}^{(\pm)}_{-1}$) and an effective dissipation $\mathrm{Im}\,\mathscr{R}^{(\pm)}_0$ ($\mathrm{Im}\,\mathscr{R}^{(\pm)}_{-1}$) for the NV ground state $|0_g\rangle$ ($|-1_g\rangle$). Taking $\mathcal{R}^{(\pm)}_0$ as an example, if $|\Gamma_{-1_g,0_e}|$ is much smaller than $|E^{(\pm)}_{-1_g,0_e}|$, then the optical Stark shift $\delta E_{0_g} \approx (\Omega_R/2)^2/\Delta^{(\pm)}_{-1_g,0_e}$ reduces to the conventional form of a second-order energy correction in non-degenerate perturbation theroy, while the dissipation $\mathrm{Im}\,\mathscr{R}^{(\pm)}_0$ takes the semiclassical form of a Fermi golden rule. Substituting Eq. (14) into Eq. (9) immediately gives $W_{m\pm1\leftarrow m}$, which assumes a tedious form as it includes various quantum coherence effects.

For simplification, we use the fact that the NV excited state dephasing $\Gamma_e \sim 10^4$ GHz $\gg$ other NV dissipation γ, γ_1, γ_φ and typical detuning $|\omega_0 - \omega|$, $|\Delta^{(\pm)}_{-1_g,0_e}|$, and $|\Delta^{(\pm)}_{-1_e,0_g}|$, and further restrict to weak optical pumping $R \ll \Gamma_{-1_e,0_e}$ (~26.3 MHz). In this case, the optical Stark shift is negligible and the optical pumping rate simplifies to $R \approx \Omega_R^2/\Gamma_e$, so the self-energies $\mathscr{R}^{(\pm)} \approx iR$ only induces NV level broadening. Substituting the resulting expression $\rho^{(\pm)}_{-1_g,0_g} \approx i/(\Delta^{(\pm)}_{-1_g,0_g} - i(\gamma_\varphi + R))$ into Eq. (9) gives

$$W_{m\pm1\leftarrow m} = P_g \xi^{\pm}_m 2\pi \left|\frac{A_{+\mp}}{2\sqrt{2}}\right|^2 \delta^{(R)}(\Delta_{m\pm1\leftarrow m}), \tag{15}$$

For spin-1/2, Eq. (15) simplifies to Eq. (2) of the main text.

Mean field method for multiple nuclear spins. The essential idea of the mean-field approximation is to assume small inter-spin correlation, so that the N-nuclei density matrix $\hat{p}$ can be factorized as $\hat{p} = \otimes_{i=1}^{N} \hat{p}_i$, where the ith nuclear spin state $\hat{p}_i \approx |\uparrow_i\rangle\langle\uparrow_i|(1 + p_i)/2 + |\downarrow_i\rangle\langle\downarrow_i|(1 - p_i)/2$ is described by its polarization p_i. This dramatically reduces the number of variables from 2^N many-nuclei populations $\{p_{\mathbf{m}}\}$ to N single-spin polarizations $\{p_i\}$. Substituting this approximation into Eq. (5) and tracing over all the nuclei except for the ith nucleus give N coupled equations:

$$\dot{p}_i = -(\overline{W}_{i,+} + \overline{W}_{i,-})\left(p_i - \frac{\overline{W}_{i,+} - \overline{W}_{i,-}}{\overline{W}_{i,+} + \overline{W}_{i,-}}\right), \tag{16}$$

where $\overline{W}_{i,\pm}$ is the spin flip rate of the ith nucleus averaged over the states of all the other $(N - 1)$ nuclear spins:

$$\begin{aligned} \overline{W}_{i,+} &= \mathrm{Tr}\, W_{i,+}(\hat{h}_z)\,|\downarrow_i\rangle\langle\downarrow_i| \otimes_{j(\neq i)} \hat{p}_j, \\ \overline{W}_{i,-} &= \mathrm{Tr}\, W_{i,-}(\hat{h}_z)\,|\uparrow_i\rangle\langle\uparrow_i| \otimes_{j(\neq i)} \hat{p}_j, \end{aligned} \tag{17}$$

i.e., $\overline{W}_{i,\pm}$ depends on the polarizations $\{p_j\}$ $(j \neq i)$ of all the other nuclear spins. Therefore, Eq. (16) with $i = 1,2,\cdots,N$ form N coupled differential equations for $\{p_i\}$. The steady-state solutions $\{p_{i,\mathrm{ss}}\}$ are obtained by solving N coupled nonlinear equations with recursive methods.

References

1. Abragam, A. *The Principles of Nuclear Magnetism* (Oxford University Press, New York, 1961).
2. Kane, B. E. A silicon-based nuclear spin quantum computer. *Nature* **393,** 133–137 (1998).
3. Gruber, A. *et al.* Scanning confocal optical microscopy and magnetic resonance on single defect centers. *Science* **276,** 2012–2014 (1997).
4. Balasubramanian, G. *et al.* Ultralong spin coherence time in isotopically engineered diamond. *Nat. Mater.* **8,** 383–387 (2009).
5. He, X.-F., Manson, N. B. & Fisk, P. T. H. Paramagnetic resonance of photoexcited n-v defects in diamond. i. level anticrossing in the 3a ground state. *Phys. Rev. B* **47,** 8809–8815 (1993).
6. Jacques, V. *et al.* Dynamic polarization of single nuclear spins by optical pumping of nitrogen-vacancy color centers in diamond at room temperature. *Phys. Rev. Lett.* **102,** 057403 (2009).
7. Maze, J. R. *et al.* Nanoscale magnetic sensing with an individual electronic spin in diamond. *Nature* **455,** 644–647 (2008).
8. Taylor, J. M. *et al.* High-sensitivity diamond magnetometer with nanoscale resolution. *Nat. Phys.* **4,** 810–816 (2008).
9. Childress, L. *et al.* Coherent dynamics of coupled electron and nuclear spin qubits in diamond. *Science* **314,** 281–285 (2006).
10. Dutt, M. V. G. *et al.* Quantum register based on individual electronic and nuclear spin qubits in diamond. *Science* **316,** 1312–1316 (2007).
11. Neumann, P. *et al.* Single-shot readout of a single nuclear spin. *Science* **329,** 542–544 (2010).
12. Togan, E., Chu, Y., Imamoglu, A. & Lukin, M. D. Laser cooling and real-time measurement of the nuclear spin environment of a solid-state qubit. *Nature* **478,** 497–501 (2011).
13. Neumann, P. *et al.* Multipartite entanglement among single spins in diamond. *Science* **320,** 1326–1329 (2008).
14. Jiang, L. *et al.* Repetitive readout of a single electronic spin via quantum logic with nuclear spin ancillae. *Science* **326,** 267–272 (2009).
15. Waldherr, G. *et al.* Quantum error correction in a solid-state hybrid spin register. *Nature* **506,** 204–207 (2014).
16. Taminiau, T. H., Cramer, J., van der Sar, T., Dobrovitski, V. V. & Hanson, R. Universal control and error correction in multi-qubit spin registers in diamond. *Nat Nano* **9,** 171–176 (2014).
17. Fischer, R. *et al.* Bulk nuclear polarization enhanced at room temperature by optical pumping. *Phys. Rev. Lett.* **111,** 057601 (2013).
18. Fischer, R., Jarmola, A., Kehayias, P. & Budker, D. Optical polarization of nuclear ensembles in diamond. *Phys. Rev. B* **87,** 125207 (2013).
19. Gali, A. Identification of individual c13 isotopes of nitrogen-vacancy center in diamond by combining the polarization studies of nuclear spins and first-principles calculations. *Phys. Rev. B* **80,** 241204 (2009).
20. Smeltzer, B., McIntyre, J. & Childress, L. Robust control of individual nuclear spins in diamond. *Phys. Rev. A* **80,** 050302 (2009).
21. Steiner, M., Neumann, P., Beck, J., Jelezko, F. & Wrachtrup, J. Universal enhancement of the optical readout fidelity of single electron spins at nitrogen-vacancy centers in diamond. *Phys. Rev. B* **81,** 035205 (2010).
22. Dréau, A., Maze, J.-R., Lesik, M., Roch, J.-F. & Jacques, V. High-resolution spectroscopy of single nv defects coupled with nearby 13c nuclear spins in diamond. *Phys. Rev. B* **85,** 134107 (2012).
23. Gaebel, T. *et al.* Room-temperature coherent coupling of single spins in diamond. *Nat. Phys.* **2,** 408–413 (2006).

24. Wang, H.-J. *et al.* Sensitive magnetic control of ensemble nuclear spin hyperpolarization in diamond. *Nat. Commun.* **4,** 1940 (2013).
25. London, P. *et al.* Detecting and polarizing nuclear spins with double resonance on a single electron spin. *Phys. Rev. Lett.* **111,** 067601 (2013).
26. Liu, G.-Q. *et al.* Protection of centre spin coherence by dynamic nuclear spin polarization in diamond. *Nanoscale* **6,** 10134–10139 (2014).
27. Alvarez, G. *et al.* Local and bulk 13c hyperpolarization in nv-centered diamonds at variable fields and orientations. *arXiv.* **1412,** 8635 (2014).
28. King, J. P. *et al.* Room-temperature *in situ* nuclear spin hyperpolarization from optically-pumped nitrogen vacancy centers in diamond. *arXiv:1501.02897* (2015).
29. Fuchs, G. D. *et al.* Excited-state spectroscopy using single spin manipulation in diamond. *Phys. Rev. Lett.* **101,** 117601 (2008).
30. Yang, W. & Sham, L. J. General theory of feedback control of a nuclear spin ensemble in quantum dots. *Phys. Rev. B* **88,** 235304 (2013).
31. Yang, W. & Sham, L. J. Collective nuclear stabilization in single quantum dots by noncollinear hyperfine interaction. *Phys. Rev. B* **85,** 235319 (2012).
32. Wang, P., Du, J. & Yang, W. Engineering nuclear spin dynamics with optically pumped nitrogen-vacancy center. *arXiv:1503.00243* (2015).
33. Hanson, R., Mendoza, F. M., Epstein, R. J. & Awschalom, D. D. Polarization and readout of coupled single spins in diamond. *Phys. Rev. Lett.* **97,** 087601 (2006).
34. Maurer, P. C. *et al.* Room-temperature quantum bit memory exceeding one second. *Science* **336,** 1283–1286 (2012).
35. Abtew, T. A. *et al.* Dynamic jahn-teller effect in the nv^- center in diamond. *Phys. Rev. Lett.* **107,** 146403 (2011).
36. Manson, N. B., Harrison, J. P. & Sellars, M. J. Nitrogen-vacancy center in diamond: Model of the electronic structure and associated dynamics. *Phys. Rev. B* **74,** 104303 (2006).
37. Robledo, L., Bernien, H., van der Sar, T. & Hanson, R. Spin dynamics in the optical cycle of single nitrogen-vacancy centres in diamond. *New J. Phys.* **13,** 025013 (2011).
38. Ma, Y., Rohlfing, M. & Gali, A. Excited states of the negatively charged nitrogen-vacancy color center in diamond. *Phys. Rev. B* **81,** 041204 (2010).
39. Choi, S., Jain, M. & Louie, S. G. Mechanism for optical initialization of spin in nv center in diamond. *Phys. Rev. B* **86,** 041202 (2012).
40. Acosta, V. M., Jarmola, A., Bauch, E. & Budker, D. Optical properties of the nitrogen-vacancy singlet levels in diamond. *Phys. Rev. B* **82,** 201202 (2010).
41. Delaney, P., Greer, J. C. & Larsson, J. A. Spin-polarization mechanisms of the nitrogen-vacancy center in diamond. *Nano Lett.* **10,** 610–614 (2010).
42. Togan, E. *et al.* Quantum entanglement between an optical photon and a solid-state spin qubit. *Nature* **466,** 730–734 (2010).
43. Loubser, J. H. N. & van Wyk, J. A. Electron spin resonance in the study of diamond. *Rep. Prog. Phys.* **41,** 1201 (1978).
44. Felton, S. *et al.* Hyperfine interaction in the ground state of the negatively charged nitrogen vacancy center in diamond. *Phys. Rev. B* **79,** 075203 (2009).
45. Greilich, A. *et al.* Nuclei-induced frequency focusing of electron spin coherence. *Science* **317,** 1896–1899 (2007).
46. Xu, X. *et al.* Optically controlled locking of the nuclear field via coherent dark-state spectroscopy. *Nature* **459,** 1105–1109 (2009).
47. Vink, I. T. *et al.* Locking electron spins into magnetic resonance by electron-nuclear feedback. *Nat. Phys.* **5,** 764–768 (2009).
48. Sun, B. *et al.* Persistent narrowing of nuclear-spin fluctuations in inas quantum dots using laser excitation. *Phys. Rev. Lett.* **108,** 187401 (2012).

Acknowledgements

This work was supported by NSFC (Grant No. 11274036 and No. 11322542) and the MOST (Grant No. 2014CB848700).

Author Contributions

W.Y. and P.W. conceived the idea, formulated the theories, analyzed the results, and wrote the paper. B.L. provided useful comments on the manuscript.

Additional Information

Competing financial interests: The authors declare no competing financial interests.

How to cite this article: Wang, P. *et al.* Strongly polarizing weakly coupled ^{13}C nuclear spins with optically pumped nitrogen-vacancy center. *Sci. Rep.* **5**, 15847; doi: 10.1038/srep15847 (2015).